



Response analysis of the composite random vibration of a high-speed elevator considering the nonlinearity of guide shoe

Rui-jun Zhang¹ · Chen Wang¹ · Qing Zhang¹

Received: 19 May 2017 / Accepted: 9 December 2017 / Published online: 20 March 2018
© The Brazilian Society of Mechanical Sciences and Engineering 2018

Abstract

As a result of unevenness (or non-uniformity) of elevator guide rails, an elevator car experiences horizontal vibration in the vertical motion of an elevator run. To improve the accuracy of the car vibration model and analyze the influence of uncertainty factors on the vibration response, the nonlinear characteristics of rolling guide shoes, randomness of car parameters, and random excitation of guide rails need to be considered. Based on the Hertz contact theory, the functional relationship between the amount of deformation of rolling guide shoes and restoring force was derived, and a nonlinear model of rolling guide shoes was established. The average responses of the composite random vibration of a high-speed elevator were determined by the orthogonal polynomial approximation method, and the standard deviations were determined by the complex Cotes integration method. With a two-degree-of-freedom high-speed elevator car system as the research object, the horizontal vibration responses were analyzed under the condition of variation of parameters and the irregularity of the guide rails. The results showed that the variation of parameters mainly affected the dispersion extent of the horizontal vibration responses of the car, and the irregularity of the guide rails mainly affected the amplitude of the vibration responses. This study provided an effective method for analyzing composite random vibration responses of a high-speed elevator car system, and provided a reference for anti-vibration design and safety assessment.

Keywords High-speed elevator · Composite random vibration · Nonlinear guide shoes · Random parameters

1 Introduction

In modern society, with the increasing height of buildings, the proportion of high-speed elevator (speed ≥ 2.5 m/s) has gradually increased to ensure efficiency. With the increase of the elevator running speed and attention to the ride comfort and safety, effectively reducing the vibration generated by the high-speed operation of the elevator has become a key issue.

In recent years, many scholars have studied transverse vibration of elevator cars. Feng et al. [1] established a dynamic model of the transverse vibration of an elevator car based on the rigid body dynamics theory, and they derived differential equations based on Newton's laws of motion and the Euler equations. Bao et al. [2] used the finite element method to establish the car frame model, and revealed the acceleration responses on the condition of dynamic loads from the perspective of transient dynamics. Chang et al. [3] established a four-degree-of-freedom elevator system to study the excitation characteristics and the car dynamic response, and developed an active mass driver based on the H_∞ direct output feedback control algorithm. Herrera et al. [4] considered the behavior of passengers in the car and established a model to analyze the influence of the car's dynamic characteristics under different loading conditions. Because the rolling guide shoe liners are made of rubber materials, its material properties give guide shoes nonlinear characteristics. For this problem, these literatures simplified guide shoes as a linear spring-damper system. The rolling guide shoes are key components that directly

Technical Editor: Kátia Lucchesi Cavalca Dedini.

✉ Rui-jun Zhang
zhangruijun@sdjzu.edu.cn

Chen Wang
wangchen1761@163.com

Qing Zhang
zhhllyq1996@163.com

¹ School of Mechanical and Electrical Engineering, Shandong Jianzhu University, Jinan 250101, China

contact the guide rails, and the nonlinear function relationship between the amounts of deformation and restoring force is bound to have an effect on the vibration responses. Thus, it is necessary to further explore the nonlinear characteristics of rolling guide shoes and apply them to the car vibration response analysis.

In addition, there are many random factors in the car system, including the randomness of the parameters and the randomness of the excitation. In the product design stage, all of the parameters are definite. However, due to the influence of actual installation circumstance, live debugging, manufacturing errors, installation errors, the influence of temperature and uncertainty of physical parameters of materials, etc., the parameters of the same batch of elevator products are different. For an actual product, its parameters are uncertain, and they present some randomness. Therefore, the actual parameters of the same specification's elevators are slightly different. The randomness of these parameters can make the vibration responses of different elevators produce variability under the same condition. The randomness of excitations is caused by the irregularity of the guide rails. To distinguish them from the time-invariant property of parameters, the excitations are time-varying, and they can affect the vibration of the car at different times. To make a more accurate vibration response analysis of a car system, the above factors must be comprehensively considered.

For the random factors that exist in the car system, the dynamic response analysis of an uncertain structure is involved. Currently, this response analysis is mainly used in the structure of building and a small number of mechanical structures, and is seldom used in the car system of high-speed elevators. Xu et al. [5] analyzed the stochastic dynamic characteristics of beams under the stochastic material properties by the random factor method. However, the authors did not combine this research with random excitation. Marcin et al. [6] solved the dynamic response of the truss structure using the Taylor expansion stochastic finite element method. The stochastic finite element method needs to set up all kinds of random parameters corresponding to the stochastic finite element characteristic matrix, and it causes much inconvenience to its computer program design. Szafran [7] analyzed the horizontal vibration responses of cable structures under the influence of a random elastic modulus and random loads by the stochastic perturbation method, and further analyzed the reliability. Although the stochastic perturbation method can quickly and easily calculate the mean and variance of the responses, it only applies to small parameter perturbation, and this method inevitably exists in secular term. That is, this method only applies to the beginning of a short period of time, and the accuracy of results quickly deteriorates with time.

For a series of problems related to the analysis of horizontal vibration responses of a high-speed elevator car system, first, the nonlinear model of rolling guide shoes was established, and then the acceleration responses of the composite random vibration of the car system were determined by the orthogonal polynomial approximation method, and the responses' standard deviations were determined by the complex Cotes precise integration method provided by Song [8]. This set of analytical methods not only avoids the secular term problem of the stochastic perturbation method but also obtains more accurate results by combining with the rolling guide shoe nonlinear model.

2 The rolling guide shoe nonlinear model

The schematic diagram of the structure of rolling guide shoe is shown in Fig. 1. The guide shoe has two elastic elements. One is the rubber lining of the roller, and the other is the spring. In the process of the traditional vibration responses analysis of a high-speed elevator car system, as an important dynamic component, the guide shoe is usually simplified as the spring-damper model. However, related research has shown that nonlinear behavior exists in the rolling guide shoe [9]. Under the effect of guide rail irregularity, the nonlinear characteristics of the guide shoes are bound to have an impact on the horizontal vibration of the car. Solving the vibration responses of the car with the spring-damping model reduces the accuracy of the solution. Taking into account the nonlinear behavior of the rolling guide shoes, in this section, the functional relationship between the amount of deformation of rolling guide shoes and the restoring force are derived by the Hertz contact theory of the elastic solid contact area [10–13].

The guide wheel and guide rail contact area are shown in Fig. 2. R is the radius of the guide wheel, L is the width of the guide wheel, F_k is the normal force of impact on the guide wheel, p is the contact stress, and a is the half-width of the contact line.

On the basis of the Hertz contact theory, the stress on the contact surface is elliptical. The stress of the contact center is the largest, marked as p_0 . The stress distribution of the remaining points is:

$$p = p_0 \sqrt{1 - \frac{x^2}{a^2}} \quad (1)$$

The volume of a semi-elliptical cylinder of stress distribution is equal to total pressure F_k , that is:

$$F_k = \frac{\pi a}{2} L p_0 \quad (2)$$

The maximum contact stress is:

Fig. 1 The schematic diagram of the structure of rolling guide shoe

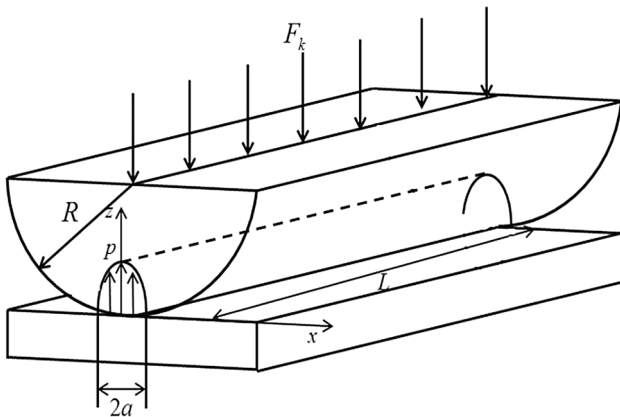
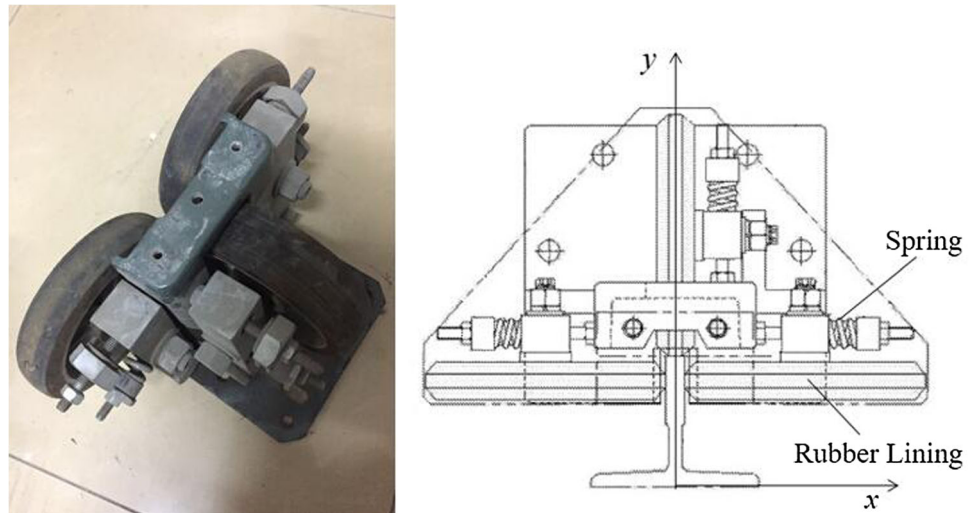


Fig. 2 The guide wheel and guide rail contact area

$$p_0 = \sigma_H = \frac{2F}{\pi a L} \tag{3}$$

The half-width a derived from the Hertz formula is:

$$a = \sqrt{\frac{4F}{\pi L} \times \frac{\frac{1-\mu_1^2}{E_1} + \frac{1-\mu_2^2}{E_2}}{\frac{1}{R_1} + \frac{1}{R_2}}} \tag{4}$$

In which, μ_1 and μ_2 are Poisson's ratio of guide wheel and guide rail, respectively, E_1 and E_2 are the elastic modulus of the guide wheel and guide rail, respectively, and R_1 and R_2 are the radius of curvature of guide wheel and guide rail, respectively. When the material of the guide wheel is rubber and the material of guide rail is steel, E_2 is much greater than E_1 and R_2 tends to infinity, thus Eq. (2) can be simplified as:

$$a = \sqrt{\frac{4F}{\pi L} \times \frac{R(1-\mu_1^2)}{E_1}} \tag{5}$$

Substituting Eq. (5) into Eq. (3), and the following equation is obtained:

$$\sigma_H = \sqrt{\frac{F}{\pi L} \times \frac{E_1}{R(1-\mu_1^2)}} \tag{6}$$

Thus, the functional relationship between rubber's deformation z_1 and pressure F is:

$$F = \left(\frac{z_1}{d}\right)^2 \pi L R (1-\mu_1^2) E \tag{7}$$

In which, d is the rubber's thickness of guide wheel. $A = \pi L R (1-\mu_1^2) E / d^2$ is set and the elastic coefficient of the spring in the guide shoe is k , so the functional relationship between the total deformation of the guide shoe and pressure F is:

$$F = kz - \left(\frac{k^3 z}{A} + \frac{k^4}{4A^2}\right)^{1/2} + \frac{k^2}{2A} \tag{8}$$

To verify the accuracy of the Eq. (7), the finite element model of guide wheel's rubber is built. The required parameters are $L = 0.05$ m, $R = 0.1$ m, $d = 0.04$ m, $\mu_1 = 0.47$, $E = 2.5e+07$ pa, and $k = 1.2e+06$ N/m. The finite element calculation result is shown in Fig. 3 and the curves of pressure change with deformation of guide wheel's rubber are shown in Fig. 4. The two curves shown in Fig. 4 are basically identical, and the accuracy of the Eq. (7) in rolling guide shoe nonlinear model. The curve of the pressure change with total deformation of the guide shoe is shown in Fig. 5. In the early part of the deformation, the main variable is the rubber of the guide shoe, thus showing the strong nonlinear characteristics. With an increase of z , the deformation of the spring on the guide shoe is dominant, the slope of the curve slowly increases, and shows near linear characteristics. Overall, the slope of the curve increases with the increase of z , which indicates that the nonlinearity of the guide shoe has a tendency to increase the vibration.

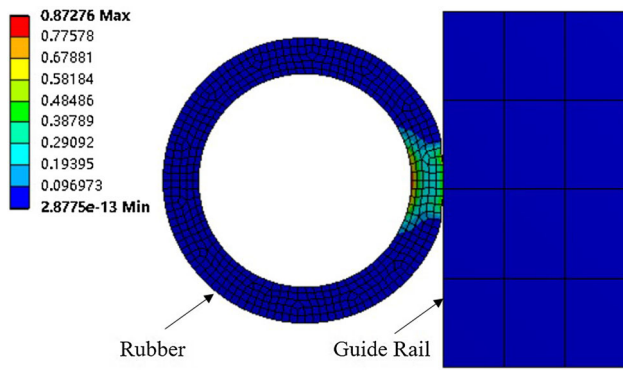


Fig. 3 The finite element calculation result (equivalent stress)

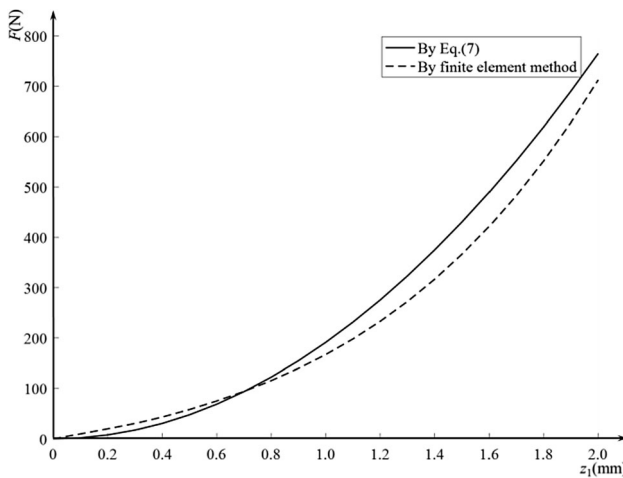


Fig. 4 The curves of pressure change with deformation of guide wheel's rubber

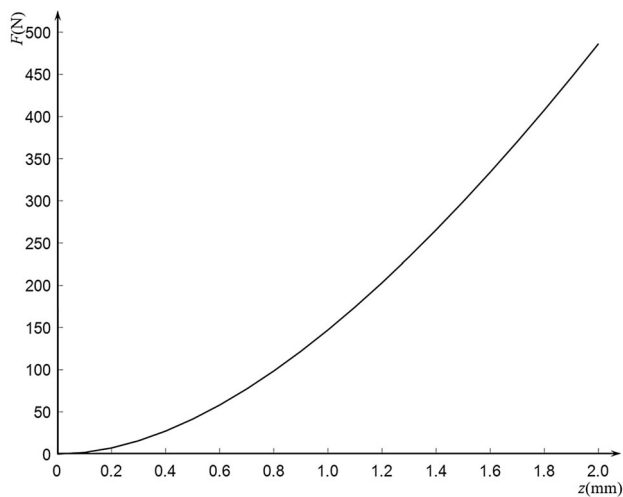


Fig. 5 Curve of the stress change with total deformation of the guide shoe

To simulate the guide rail irregularities, random excitations were constructed by superimposing Gauss white noises on deterministic pulse excitations, as shown in

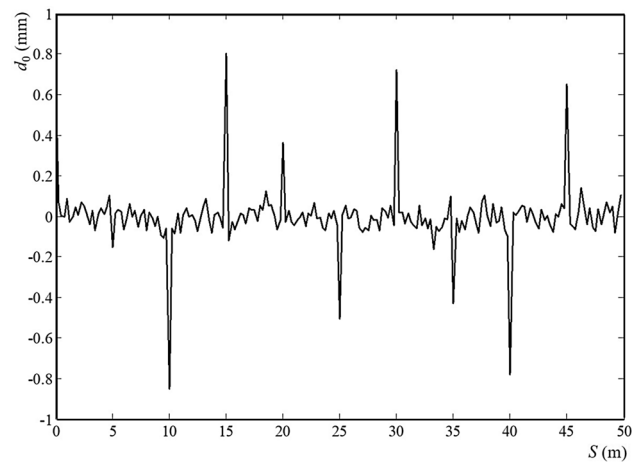


Fig. 6 Guide rail irregularity curve

Fig. 6. The S is the vertical displacement of the elevator. The d_0 represents the horizontal deviation between the actual guide rail and the ideal guide rail. Because of the pretightening force in the rolling guide shoe, the roller of the guide shoe is always in contact with the guide rail, so the d_0 is equivalent to z . The pulse excitations were caused by common guide rail joint irregularities, and the length of a single guide rail was 5 m. The Gauss white noises were caused by small fluctuations of the guide rail surface and guide wheel surface, and the standard deviation was 0.05. Figures 8 and 9 show the random waveform established by the nonlinear guide shoes and the traditional linear guide shoes, in which, the stiffness of linear guide shoes is fitted by the curve of Fig. 5 (The comparison between nonlinear and linear guide shoe model is shown in Fig. 7). Comparing with Figs 8 and 9, in the larger amplitude pulse points, the exciting forces are larger than that of the linear model, and this is bound to aggravate the vibration responses of the car. Between the two joints of the guide rail, the surface is relatively smooth. Because the initial slope of the F - z curve of the nonlinear guide shoe model is smaller than that of the linear model, the amplitude of the former is smaller than that of the latter. But the differences can be ignored because they are very small.

3 The dynamic analysis of a car system based on the orthogonal polynomial approximation method

This section uses the orthogonal polynomial approximation method dealing with the randomness of parameters in a car system [14–16]. This method can solve problems according to the following. In random function space, first, the responses are expanded into the generalized Fourier series according to a standard orthogonal basis. Then, the random

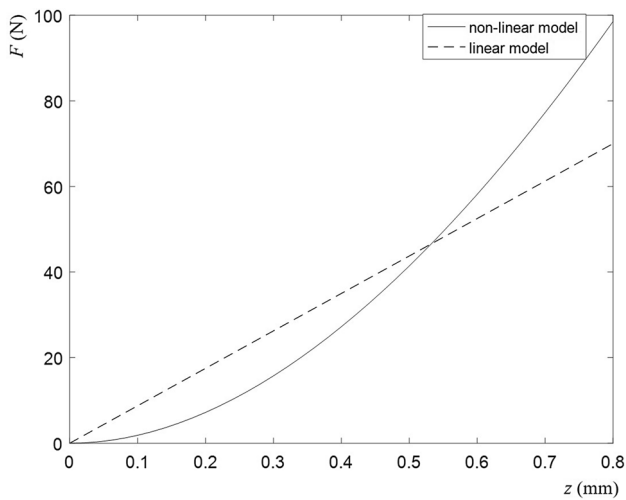


Fig. 7 The comparison between nonlinear and linear guide shoe model

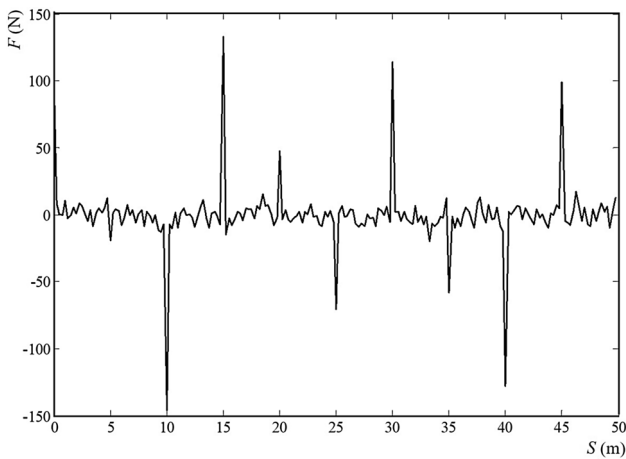


Fig. 8 Guide rail excitations by the nonlinear model

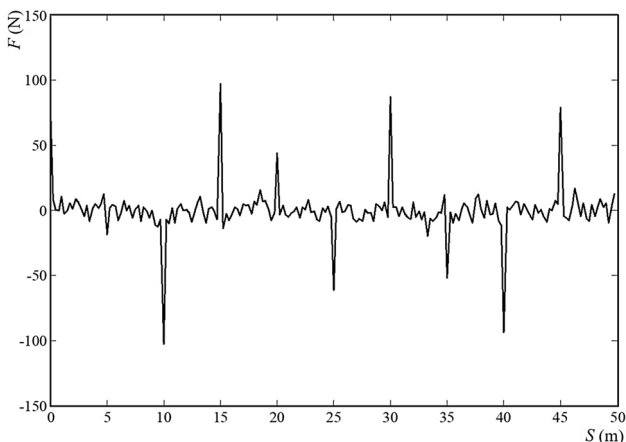


Fig. 9 Guide rail excitations by the linear model

system is converted into the equivalent determinacy system by utilizing the inner product properties of standard orthogonal basis functions. This method is not affected by large parameter perturbations and can avoid the adverse effects of the secular terms of the stochastic perturbation method.

3.1 Orthogonal decomposition of the random function

Let $\{H_i(\xi), i = 1, 2, 3 \dots\}$ be a cluster of the orthogonal function system. For random variables with a normal distribution, the Hermite polynomials can be functions of the orthogonal system. For random variables with a uniform distribution, the Legendre polynomials can be functions of the orthogonal system [17]. For random variables with an exponential distribution [18], the Laguerre polynomials can be functions of the orthogonal system [19]. $p(\xi)$ as a probability density distribution function of ξ , together with $H_i(\xi)$ satisfies the following equation:

$$\int_{\Omega} p(\xi)H_m(\xi)H_n(\xi) = \delta_{mn}h_m \tag{9}$$

In which, Ω is the definitional domain of the real variable ξ and δ_{mn} is the Kronecker delta.

Equation (9) is the weighted orthogonal relation of the orthogonal functions system. In addition, the orthogonal function system also has the following recurrence relation:

$$\xi H_n(\xi) = \alpha_n H_{n-1}(\xi) + \beta_n H_n(\xi) + \gamma_n H_{n+1}(\xi) \tag{10}$$

If all the Cauchy sequence of points in the random function space are convergent, any function in this space can be expanded into the following series:

$$f(\xi) = \sum_{i=0}^{\infty} a_i H_i(\xi) \tag{11}$$

In which

$$a_i = \int_{\Omega} p(\xi)f(\xi)H_i(\xi)dx \tag{12}$$

Equation (11) is the orthogonal expansion of the random function $f(\xi)$ and it is the basis of the orthogonal polynomial approximation method.

3.2 Analysis of horizontal vibration responses of a high-speed elevator

For a high-speed elevator system with random parameters under random excitations, its dynamic differential equations can be expressed as:

$$M\ddot{X} + C\dot{X} + KX = F(t) \tag{13}$$

In which, M , C , and K are the mass matrix, damping matrix, and stiffness matrix respectively, $F(t)$ is the external excitation vector, and X is the displacement response. When the M , C , K , and $F(t)$ are random parameters, this system becomes a composite random system. Then, converting Eq. (13) into the expression of the collection of independent random variables:

$$\left(M_0 + \sum_{i=1}^{N_m} M_i \zeta_i \right) \ddot{X} + \left(C_0 + \sum_{i=1}^{N_c} C_i \zeta_i \right) \dot{X} + \left(K_0 + \sum_{i=1}^{N_k} K_i \zeta_i \right) X = F(t) \tag{14}$$

In which, N_m , N_c , and N_k are the number of independent random variables of the mass matrix, damping matrix, and stiffness matrix, respectively. The total number of random variables is:

$$R = N_m + N_c + N_k. \tag{15}$$

The subscript 0 indicates the mean of M , C , and K . The subscript i indicates the corresponding standard deviation coefficient matrix. ζ_i is a random variable which obeys arbitrary distribution. According to the orthogonal decomposition, the responses X , \dot{X} , and \ddot{X} are expanded to the series of the orthogonal basic functions:

$$X(\xi) = \sum_{n_1=0}^{N_1-1} \dots \sum_{n_R=0}^{N_R-1} Y_{n_1 n_2 \dots n_R} H_{n_1}(\xi_1) \dots H_{n_R}(\xi_R) \tag{16}$$

$$\dot{X}(\xi) = \sum_{n_1=0}^{N_1-1} \dots \sum_{n_R=0}^{N_R-1} \dot{Y}_{n_1 n_2 \dots n_R} H_{n_1}(\xi_1) \dots H_{n_R}(\xi_R) \tag{17}$$

$$\ddot{X}(\xi) = \sum_{n_1=0}^{N_1-1} \dots \sum_{n_R=0}^{N_R-1} \ddot{Y}_{n_1 n_2 \dots n_R} H_{n_1}(\xi_1) \dots H_{n_R}(\xi_R) \tag{18}$$

Equations (16–18) are substituted into Eq. (14), and the following formula is obtained by utilizing Eq. (10).

$$\begin{aligned} & \left(M_0 \frac{d^2}{dt^2} + C_0 \frac{d}{dt} + K_0 \right) \sum_{n_1=0}^{N_1-1} \dots \sum_{n_R=0}^{N_R-1} Y_{N_1 N_2 \dots N_R} H_{n_1}(\xi_1) \dots H_{n_R}(\xi_R) \\ & + \sum_{i=1}^{N_m} M_i \sum_{n_1=0}^{N_1-1} \dots \sum_{n_R=0}^{N_R-1} \mathcal{Y}_{N_1 N_2 \dots N_R} H_{n_1}(\xi_1) \dots H_{n_{i-1}}(\xi_{i-1}) \\ & \times [\alpha_{n_i} H_{n_i-1}(\xi_i) + \beta_{n_i} H_{n_i}(\xi_i) + \gamma_{n_{i+1}} H_{n_{i+1}}(\xi_i)] H_{n_{i+1}}(\xi_{i+1}) \dots H_{n_R}(\xi_R) \\ & + \sum_{i=1}^{N_c} C_i \sum_{n_1=0}^{N_1-1} \dots \sum_{n_R=0}^{N_R-1} \dot{Y}_{N_1 N_2 \dots N_R} H_{n_1}(\xi_1) \dots H_{n_{i-1}}(\xi_{i-1}) \\ & \times [\alpha_{n_i} H_{n_i-1}(\xi_i) + \beta_{n_i} H_{n_i}(\xi_i) + \gamma_{n_{i+1}} H_{n_{i+1}}(\xi_i)] H_{n_{i+1}}(\xi_{i+1}) \dots H_{n_R}(\xi_R) \\ & + \sum_{i=1}^{N_k} K_i \sum_{n_1=0}^{N_1-1} \dots \sum_{n_R=0}^{N_R-1} Y_{N_1 N_2 \dots N_R} H_{n_1}(\xi_1) \dots H_{n_{i-1}}(\xi_{i-1}) \\ & \times [\alpha_{n_i} H_{n_i-1}(\xi_i) + \beta_{n_i} H_{n_i}(\xi_i) + \gamma_{n_{i+1}} H_{n_{i+1}}(\xi_i)] H_{n_{i+1}}(\xi_{i+1}) \dots H_{n_R}(\xi_R) \\ & = F(t) \end{aligned} \tag{19}$$

Both ends of Eq. (19) are multiplied by $H_{r_1}(\xi_1) \dots H_{r_R}(\xi_R)$,

and the following formula is obtained by utilizing the weighted orthogonal relation Eq. (9).

$$\begin{aligned} & \left(M_0 \frac{d^2}{dt^2} + C_0 \frac{d}{dt} + K_0 \right) Y_{r_1 r_2 \dots r_R} \\ & + \sum_{i=1}^R M_i [\alpha_{r_{i+1}} \mathcal{Y}_{r_1 r_2 \dots r_{i-1} r_{i+1} r_{i+1} \dots r_R} + \beta_{r_i} \mathcal{Y}_{r_1 r_2 \dots r_R} \\ & + \gamma_{r_{i-1}} \mathcal{Y}_{r_1 r_2 \dots r_{i-1} r_{i-1} r_{i-1} \dots r_R}] + \sum_{i=1}^R C_i [\alpha_{r_{i+1}} \dot{Y}_{r_1 r_2 \dots r_{i-1} r_{i+1} r_{i+1} \dots r_R} \\ & + \beta_{r_i} \dot{Y}_{r_1 r_2 \dots r_R} + \gamma_{r_{i-1}} \dot{Y}_{r_1 r_2 \dots r_{i-1} r_{i-1} r_{i-1} \dots r_R}] \\ & + \sum_{i=1}^R K_i [\alpha_{r_{i+1}} Y_{r_1 r_2 \dots r_{i-1} r_{i+1} r_{i+1} \dots r_R} + \beta_{r_i} Y_{r_1 r_2 \dots r_R} \\ & + \gamma_{r_{i-1}} Y_{r_1 r_2 \dots r_{i-1} r_{i-1} r_{i-1} \dots r_R}] = F(t) \delta_{0r_1} \delta_{0r_2} \dots \delta_{0r_R} \end{aligned} \tag{20}$$

After every $r_i (i = 1, 2, \dots, R)$ of $H_{r_1}(\xi_1) \dots H_{r_R}(\xi_R)$ is taken over all $r_i = 0, 1, \dots, N_i - 1$, $\prod_{i=1}^R N_i$ deterministic equations of responses $Y = [Y_{00 \dots 0} Y_{00 \dots 1} \dots Y_{N_1-1 N_2-1 \dots N_R-1}]^T$ are obtained. At this point, a random dynamic equation with n degrees of freedom is converted into an equivalent extended-order deterministic system dynamic equation with $\prod_{i=1}^R N_i$ degrees of freedom. To obtain the response of the original system, the components of Y are substituted into Eqs. (16–18).

The standard deviations of the extended-order system dynamic responses under the random excitation $F(t)$ are obtained by the complex Cotes integration method suggested by [8].

4 Example analysis

In this section, a two-degree-of-freedom high-speed elevator car system vibration model was used as an example (refer to [20]), and the vibration responses of the car and the numerical characteristics of responses were analyzed. As shown in Fig. 10, a rectangular coordinate system was established. The elevator car’s centroid o is the origin, and the horizontal direction and the plumb direction are the x axis and y axis, respectively. The elevator car has two degrees of freedom, and they are the translation of the horizontal direction and the rotation around the centroid on the oxy surface. The mass of the elevator car is m , the moment of inertia is J , the stiffness of the spring in the guide shoes is k , and the damping of the guide shoes is c . The distance from the upper guide shoes to the mass is l_1 and the distance from the lower guide shoes to the mass is l_2 . For the values of the car’s parameters refer to [20]. The calculation results of [20] showed that the sensitivity of geometric parameters l_1 and l_2 were much greater than that

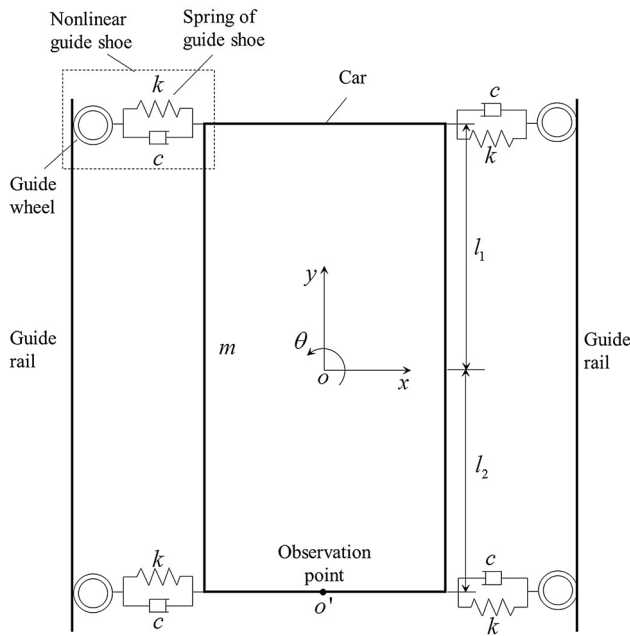


Fig. 10 Vibration model of the two-degrees-of-freedom car system

of the quality parameters m and J and kinetic parameters k and c . That is, under the same coefficient of variation, the influences of the randomness of parameters l_1 and l_2 on the responses are much larger than the other parameters. Therefore, the car mass m , the moment of inertia J , the stiffness of the spring k , and the damping of guide shoes c are considered as deterministic parameters. Their values are $m = 1000 \text{ kg}$, $J = 1500 \text{ kg m}^2$, $k = 7500 \text{ N/m}$ and $c = 120 \text{ N/(m/s)}$. The geometric parameters are considered as random parameters. The mean values of l_1 and l_2 are $\bar{l}_1 = 1.6 \text{ m}$ and $\bar{l}_2 = 1.4 \text{ m}$. In this case, the coefficient of variation is 0.05, the standard deviations $\sigma_{l_1} = 0.08 \text{ m}$, and $\sigma_{l_2} = 0.07 \text{ m}$.

The dynamical differential equations of this system are shown below

$$M\ddot{X} + C\dot{X} + KX = F(t) \tag{21}$$

In which

$$M = \begin{pmatrix} m & 0 \\ 0 & J \end{pmatrix}, \quad C = \begin{pmatrix} 4c - 2c(l_1 - l_2) & \\ -2c(l_1 - l_2) & 2c(l_1^2 + l_2^2) \end{pmatrix},$$

$$K = \begin{bmatrix} 4k - 2k(l_1 - l_2) & \\ -2k(l_1 - l_2) & 2k(l_1^2 + l_2^2) \end{bmatrix} X = \begin{pmatrix} x \\ \theta \end{pmatrix}$$

$F(t)$ is the external excitation vector caused by the irregularity of the guide rails in the car system shown in Fig. 8.

The stiffness matrix and damping matrix of the differential equation of the car vibration system can be written as the following equations:

$$K = K_0 + K_1\xi_1 + K_2\xi_2 \tag{22}$$

$$C = C_0 + C_1\xi_1 + C_2\xi_2 \tag{23}$$

In which $K_0 = \begin{bmatrix} 4k & -2k(\bar{l}_1 - \bar{l}_2) \\ -2k(\bar{l}_1 - \bar{l}_2) & 2k(\bar{l}_1^2 + \bar{l}_2^2) \end{bmatrix}$, $K_1 = \begin{bmatrix} 0 & -2k \\ -2k & 4k\bar{l}_1 \end{bmatrix} \sigma_{l_1}$, $K_2 = \begin{bmatrix} 0 & 2k \\ 2k & 4k\bar{l}_2 \end{bmatrix} \sigma_{l_2}$, $C_0 = \begin{bmatrix} 4c & -2c(\bar{l}_1 - \bar{l}_2) \\ -2c(\bar{l}_1 - \bar{l}_2) & 2c(\bar{l}_1^2 + \bar{l}_2^2) \end{bmatrix}$, $C_1 = \begin{bmatrix} 0 & -2c \\ -2c & 4c\bar{l}_1 \end{bmatrix} \sigma_{l_1}$, $C_2 = \begin{bmatrix} 0 & 2c \\ 2c & 4c\bar{l}_2 \end{bmatrix} \sigma_{l_2}$. The ξ_1 and ξ_2 obey the standard normal distribution. Equation (21) can be written as:

$$M\ddot{X} + (C_0 + C_1\xi_1 + C_2\xi_2)\dot{X} + (K_0 + K_1\xi_1 + K_2\xi_2)X = F(t). \tag{24}$$

According to the orthogonal polynomial approximation method, the responses of a system are decomposed in accordance with three-order Hermite polynomials.

$$X(\xi) = \sum_{n_1=0}^3 \dots \sum_{n_R=0}^3 Y_{n_1 n_2} H_{n_1}(\xi_1) H_{n_2}(\xi_2) \tag{25}$$

$$\dot{X}(\xi) = \sum_{n_1=0}^3 \dots \sum_{n_R=0}^3 \dot{Y}_{n_1 n_2} H_{n_1}(\xi_1) H_{n_2}(\xi_2) \tag{26}$$

$$\ddot{X}(\xi) = \sum_{n_1=0}^3 \dots \sum_{n_R=0}^3 \ddot{Y}_{n_1 n_2} H_{n_1}(\xi_1) H_{n_2}(\xi_2) \tag{27}$$

where $H_{n_1}(\xi_1)$ and $H_{n_2}(\xi_2)$ are the corresponding order Hermite polynomials. Substituting Eqs. (25–27) into Eq. (24) and utilizing the weighted orthogonal relation to rearrange it, a 32-order deterministic vibration differential equation can be obtained

$$M_{(32 \times 32)} \ddot{Y} + C_{(32 \times 32)} \dot{Y} + K_{(32 \times 32)} Y = F_{(32 \times 1)}(t) \tag{28}$$

Equation (28) can be solved by the Wilson- θ numerical integration method. The responses of the original system can be obtained by substituting the responses of the extended-order system into Eqs. (25–27). In this paper, the center point of car bottom is regarded as observation point o' . The acceleration mean responses of the observation point were calculated in the case of the irregularity of the guide rails as shown in Fig. 6, and compared with the results obtained by Monte Carlo method, as shown in Fig. 11.

As can be seen from Fig. 11, the curve obtained by this method is in good agreement with the Monte Carlo method. It suggests that this method has high precision. On the graph, the point of the sharp change of acceleration is located at the junctions of the guide rail, and the direction of acceleration is the same as the deviation direction of the guide rail junctions, which is in accordance with the actual

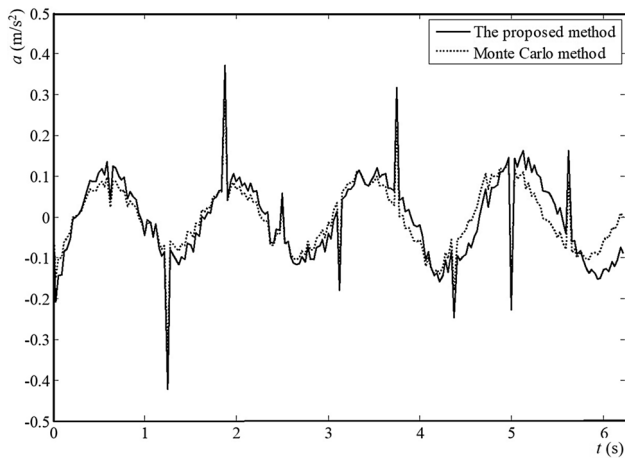


Fig. 11 Mean horizontal vibration acceleration responses of the observation point

situation. After removing the points of guide rail joints, the car is similar to a harmonic vibration, and the non-smooth shape of the wave is caused by the irregularity of the guide rails' surface.

The mean responses of the horizontal acceleration at the observation point of the car were calculated by the random excitations of Figs. 8 and 9, respectively, and the resulting contrast images are shown in Fig. 12. The random excitations of the former were produced in the nonlinear guide shoe model, and the random excitations of the latter were produced in traditional linear guide shoe model. It can be seen that the mean responses of the former are generally greater than the latter. This is especially evident in the guide rail junctions. This is further verified by the result obtained from the analysis of Fig. 5 in Sect. 2: the non-linearity of the guide shoes will aggravate the vibration of the car.

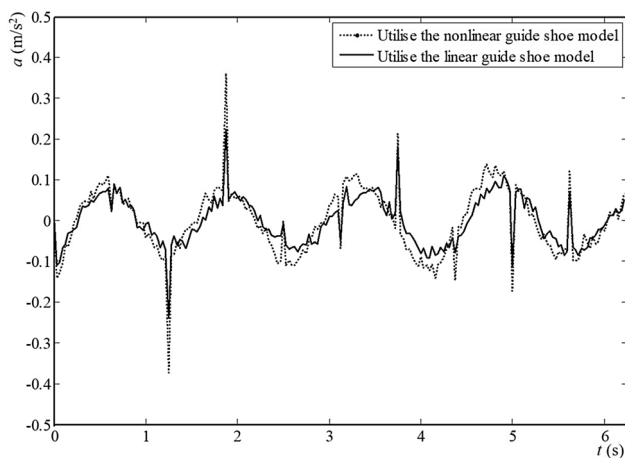


Fig. 12 Mean acceleration responses obtained by the nonlinear guide shoe model and linear guide shoe model

To study the influence of different C_v (coefficient of variation) of parameters on the mean horizontal acceleration responses of the observation point, the mean responses of acceleration were calculated in the case of the C_v of the car parameters equal to 0.05 and 0.005, respectively, and the resulting image is shown in Fig. 13. Comparing the two curves of Fig. 13, under the low coefficient of variation, the acceleration response amplitudes of the observation point are slightly lower than those under the high coefficient of variation. This shows that reducing only the variability of random parameters has little effect on reducing the horizontal vibration acceleration of the car. The standard deviations of the acceleration responses were calculated, and the results are shown in Table 1. Ten equally spaced time points are chosen as the object of inspection. The coefficient of variation of responses are obtained by calculating means and standard deviations of the responses. After calculation, the difference of their means is small, but the values of standard deviations of the latter are on average 8.1 times that of the former, and the coefficient of variation of the latter are on average 3 times that of the former. This shows that reducing the variability of random parameters has a great effect on reducing the degree of dispersion of acceleration responses.

When the irregularity of the guide rails was lowered, the acceleration responses at the observation point were calculated, and compared with the original acceleration responses. The results are shown in Fig. 14. The irregularity of the guide rail was reduced to 0.5 times the original, and the vibration acceleration response amplitudes of the observation point were obviously smaller than the amplitudes of the original vibration responses. This shows that improving the straightness and flatness of the guide rails can effectively reduce the horizontal vibration of the car.

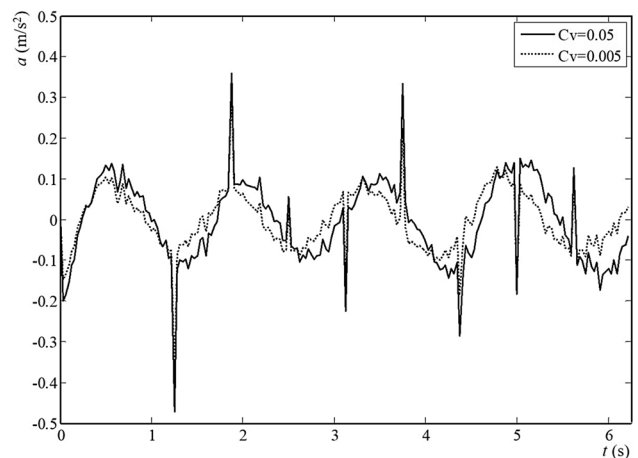
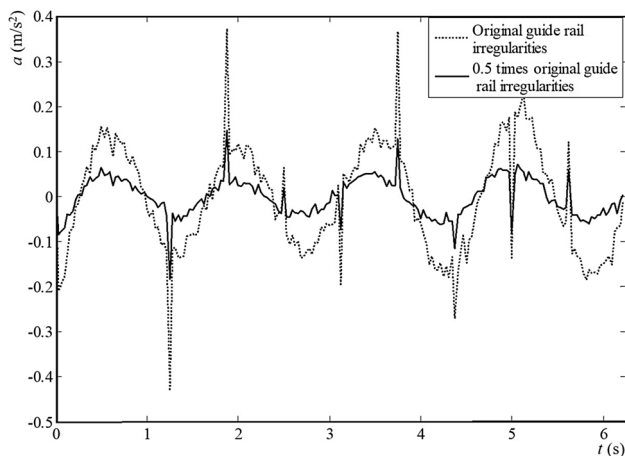


Fig. 13 Mean horizontal vibration acceleration responses of the observation point at different coefficients of variation

Table 1 Numerical characteristics of responses in the case of the same random excitation and different parameters' C_v

Time (s)	0.625	1.250	1.875	2.500	3.125	3.750	4.375	5.000	5.625	6.250
Parameters' C_v equal to 0.005										
Mean (m/s^2)	0.0832	-0.0728	0.0670	-0.0673	0.0433	-0.0012	-0.0473	0.0801	-0.0575	0.0104
SD (m/s^2)	0.0013	0.0013	0.0014	0.0015	0.0031	0.0024	0.0027	0.0023	0.0017	0.0032
C_v	0.0156	0.0178	0.0210	0.0222	0.0716	2.000	0.0571	0.0287	0.0296	0.3077
Parameters' C_v equal to 0.05										
Mean (m/s^2)	0.0849	-0.0738	0.0670	-0.0645	0.0381	0.0061	-0.0586	0.0917	-0.0679	0.0166
SD (m/s^2)	0.0036	0.0022	0.0087	0.0166	0.0236	0.0304	0.0309	0.0272	0.0153	0.0099
C_v	0.0424	0.0298	0.1299	0.2574	0.6194	4.9836	0.5273	0.2966	0.2253	0.5964

**Fig. 14** Mean vibration acceleration responses at the original and 0.5 times the original irregularity of the guide rails

5 Conclusions

- (1.) To make the model closer to the actual situation, in this paper, the shortcomings of the linear guide shoe model were avoided in the analysis of the horizontal vibration of a traditional high-speed elevator car. The functional relationship between the amount of deformation of the rolling guide shoes and the restoring force were derived by the Hertz contact theory, and the nonlinear guide shoe model was established. Under the same random irregularity of the guide rails, random guide rail excitations generated by these two models were compared and analyzed. It was concluded that the nonlinearity of the rolling guide shoes can aggravate the vibration of the car.
- (2.) The response analysis method of composite random vibration of a high-speed elevator was established by the orthogonal polynomial approximation method, and the horizontal vibration acceleration responses

of a two-degree-freedom car model were analyzed and calculated. The acceleration diagram obtained by this method can well fit the acceleration diagram obtained by Monte Carlo method, and the accuracy of the method used in this paper is verified.

- (3.) Under the different parameters' coefficients of variation and different irregularities of the guide rails, the horizontal vibration acceleration responses of high-speed elevator car system were compared and analyzed. The results showed that reducing the random parameters' coefficient of variation can greatly reduce the dispersion degree in the mean of responses, but it can not effectively reduce the amplitude of the mean vibration acceleration responses, but reducing the irregularity of the guide rails (increasing the flatness and straightness of the guide rail) can greatly reduce the vibration acceleration of the car.

Acknowledgements This work was supported by the Shandong Jianzhu University Doctor Foundation [grant umbers XNBS1514], Natural Foundation of Shandong Province [ZR2017MEE049] and research project “The research on the key techniques of a green high-speed elevator”.

References

1. Feng YH, Zhang JW (2009) Modeling and robust control of horizontal vibrations for high-speed elevator. *J Vib Control* 15(9):1375–1396. <https://doi.org/10.1177/1077546308096102>
2. Yuan BAO, Hong-liang LI (2014) Finite-element-based dynamical analysis on high-speed elevator car frame. *Chin J Constr Mach* 12(2):127–131. <https://doi.org/10.3969/j.issn.1672-5581.2014.02.008>
3. Chang CC, Lin CC, Su WC et al (2011) H_∞ Direct output feedback control of high-speed elevator systems. In: *Proceedings of the ASME 2011 pressure vessels & piping division conference, USA, 2011*: pp 289–296. <https://doi.org/10.1115/pvp2011-57814>
4. Herrera I, Su H, Kaczmarczyk S (2015) Influence of the load occupancy ratio on the dynamic response of an elevator car system. *Appl Mech Mater* 706:128–136

5. Xu Y, Qian Y, Chen JJ et al (2015) Stochastic dynamic characteristics of FGM beams with random material properties. *Compos Struct* 133:585–594. <https://doi.org/10.1016/j.compstruct.2015.07.057>
6. Kaminski M, Solecka M (2013) Optimization of the truss-type structures using the generalized perturbation-based stochastic finite element method. *Finite Elem Anal Des* 63:69–79. <https://doi.org/10.1016/j.finel.2012.08.002>
7. Szafran J (2015) Application of the generalized stochastic perturbation method in cable structures analysis. *Struct Environ* 7(2): 61–71. http://www.sae.tu.kielce.pl/23/S&E_NR_23_Art_2.pdf
8. Song X, An W, Jiang Y (2013) A numerical method for random vibration analysis of structures under arbitrary random excitations. *J Vib Shock* 32(13):147–169. <https://doi.org/10.13465/j.cnki.jvs.2013.13.007>
9. Zhang X, Li H, Meng G (2011) Experimental research of frictional characteristics on slide guide of elevator systems. *J Mech Strength*. 33(4):528–533. <https://doi.org/10.16579/j.issn.1001.9669.2011.04.024>
10. Hu X, Song B, Dai X et al (2016) Research of gear contact based on Hertz contact theory. *J Zhejiang Univ Technol* 44(1):19–22. <https://doi.org/10.3969/j.issn.1006-4303.2016.01.005>
11. Sadeghi J, Khajehdezfuly A, Esmaili M et al (2016) Dynamic interaction of vehicle and discontinuous slab track considering nonlinear hertz contact model. *J Transp Eng* 142(4):1–11. [https://doi.org/10.1061/\(ASCE\)TE.1943-5436.0000823](https://doi.org/10.1061/(ASCE)TE.1943-5436.0000823)
12. Machado M, Moreira P, Flores P et al (2012) Compliant contact force models in multibody dynamics : evolution of the Hertz contact theory. *Mech Mach Theory* 53(7):99–121. <https://doi.org/10.1016/j.mechmachtheory.2012.02.010>
13. Axinte T (2013) Hertz contact problem between wheel and rail. *Adv Mater Res* 837:733–738. <https://doi.org/10.4028/www.scientific.net/AMR.837.733>
14. Rahman S, Yadav V (2011) Orthogonal polynomial expansions for solving random eigenvalue problems. *Int J Uncertain Quantif* 1(2):163–187. <https://doi.org/10.1615/Int.J.UncertaintyQuantification.v1.i2.40>
15. Provost SB, Ha HT (2015) Distribution approximation and modelling via orthogonal polynomial sequences. *Statistics* 50(2):454–470. <https://doi.org/10.1080/02331888.2015.1053809>
16. Liu J, Sun XingsXheng, Han X et al (2015) Dynamic load identification for stochastic structures based on Gegenbauer polynomial approximation and regularization method. *Mech Syst Signal Process* 56–57:35–54. <https://doi.org/10.1016/j.ymssp.2014.10.008>
17. Wong MW (1998) Weyl transforms. Springer, New York, pp 87–91. https://doi.org/10.1007/0-387-22778-4_18
18. Bos L, Narayan A, Levenberg N et al (2015) An orthogonality property of the legendre polynomials. *Construct Approx* 45:65–81. <https://doi.org/10.13140/rg.2.1.3605.3929>
19. Kim T, Kim DS, Hwang KW et al (2016) Some identities of Laguerre polynomials arising from differential equations. *Mech Syst Signal Process* 2016(1):1–9. <https://doi.org/10.1186/s13662-016-0896-1>
20. Zhang R, Si X, Yang W et al (2015) Resonance reliability sensitivity for a high-speeding elevator cabin system with random parameters. *J Vib Shock* 34(6):84–88. <https://doi.org/10.13465/j.cnki.jvs.2015.06.016>